INTERNATIONAL JOURNAL OF HYDROGEN ENERGY XXX (XXXX) XXX

Available online at www.sciencedirect.com

ScienceDirect

journal homepage: www.elsevier.com/locate/he

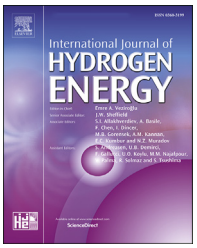

Development of risk mitigation guidance for sensor placement inside mechanically ventilated enclosures – Phase 1

Andrei V. Tchouvelev [a,*], *William J. Buttner* [b], *Daniele Melideo* [c], *Daniele Baraldi* [c], *Benjamin Angers* [d]

[a] A.V. Tchouvelev & Associates Inc., 6591 Spinnaker Cir, Mississauga, ON, Canada
[b] National Renewable Energy Laboratories, Golden, CO, USA
[c] EC Joint Research Centre, Petten, Netherlands
[d] Hydrogen Research Institute, Université Du Québec à Trois-Rivières, QC, Canada

HIGHLIGHTS

- The philosophy of approach to the role of sensors for risk reduction and mitigation.
- He tests inside an industrial enclosure containing real hydrogen equipment.
- CFD modeling performed by two independent international teams.
- Draft guidance for H_2 sensor placement inside mechanically ventilated enclosures.
- Outline of future work in this area of research.

ARTICLE INFO

Article history:
Received 6 March 2020
Received in revised form
14 September 2020
Accepted 15 September 2020
Available online xxx

Keywords:
risk mitigation
guidance for sensor placement
mechanically ventilated enclosures
hydrogen safety
regulations codes and standards

ABSTRACT

Guidance on Sensor Placement was identified as the top research priority for hydrogen sensors at the 2018 HySafe Research Priority Workshop on hydrogen safety in the category Mitigation, Sensors, Hazard Prevention, and Risk Reduction. This paper discusses the initial steps (Phase 1) to develop such guidance for mechanically ventilated enclosures. This work was initiated as an international collaborative effort to respond to emerging market needs related to the design and deployment equipment for hydrogen infrastructure that is often installed in individual equipment cabinets or ventilated enclosures. The ultimate objective of this effort is to develop guidance for an optimal sensor placement such that, when integrated into a facility design and operation, will allow earlier detection at lower levels of incipient leaks, leading to significant hazard reduction. Reliable and consistent early warning of hydrogen leaks will allow for the risk mitigation by reducing or even eliminating the probability of escalation of small leaks into large and uncontrolled events. To address this issue, a study of a real-world mechanically ventilated enclosure containing GH_2 equipment was conducted, where CFD modeling of the hydrogen dispersion (performed by AVT and UQTR, and independently by the JRC) was validated by the NREL Sensor laboratory using a Hydrogen Wide Area Monitor (HyWAM) consisting of a 10-point gas and temperature measurement analyzer. In the release test, helium was used as a hydrogen surrogate. Expansion of indoor releases to other larger facilities (including parking structures, vehicle maintenance facilities and potentially tunnels) and incorporation into QRA tools, such as HyRAM is planned for Phase 2. It is anticipated that results of this work will

* *Corresponding author*. A.V. Tchouvelev & Associates Inc., 6591 Spinnaker Cir, Mississauga, ON, Canada.
E-mail address: atchouvelev@tchouvelev.org (A.V. Tchouvelev).
https://doi.org/10.1016/j.ijhydene.2020.09.108

be used to inform national and international standards such as NFPA 2 Hydrogen Technologies Code, Canadian Hydrogen Installation Code (CHIC) and relevant ISO/TC 197 and CEN documents.

Introduction

Hydrogen safety sensors are used because of their ability to respond to unintentional hydrogen releases, which would otherwise be undetectable by human senses alone. NFPA 2 [1], CHIC [2] and the International Fire Code [3] explicitly prescribe the use of hydrogen sensors for many hydrogen operations. Thus, the use of hydrogen sensors is legally mandated within those jurisdictions that have formally adapted either NFPA 2, CHIC or the IFC, which will be the case for most jurisdictions within the United States and Canada. It should also be noted that ISO 19880−1 [4] standard covering general requirements for gaseous hydrogen fueling stations recommends using hydrogen detection to control and mitigate potential hydrogen leaks. Hence, even if not mandated by legally binding code requirements, hydrogen sensors as part of detection apparatus or system are frequently used to assure appropriate Safety Integrity Levels (SIL) in a hydrogen facility. The actual deployment of hydrogen sensors has, however, been more intuitive than scientific, and their placement and operation are not necessarily optimized for maximum safety assurance as there has been little guidance on how to optimally integrate hydrogen sensors into a facility design.

Guidance on the proper placement of hydrogen safety sensors was identified as the top research priority for hydrogen sensors in the session *Mitigation, Sensors, Hazard Prevention, and Risk Reduction* [5] at the recent HySafe Research Priority Workshop (RPW) [6]. This was consistent with the performance gap analysis from a recent international hydrogen sensor workshop [7] co-organized by personnel from the sensor laboratories at the Joint Research Center (JRC) [8] and NREL [9], in conjunction with the Fuel Cell and Hydrogen Joint Undertaking (FCH JU). Participants at the 2018 HySafe RPW comprised an international team of experts on various aspects of hydrogen safety. Of the various gaps identified pertaining to hydrogen sensors during the RPW, nearly 80% of the voting participants identified guidance on sensor placement as the most critical research gap (100% of the participants identified placement guidance to be within the top three research gaps). One outcome of the HySafe RPW was the recognition of the interrelationship between released hydrogen behaviour and sensor placement for effective active monitoring as a risk mitigation strategy, and that the elucidation of hydrogen dispersion models can guide the facility design and operation with improved safety.

The focus of the research described in this paper is to elucidate hydrogen dispersion behaviour for indoor releases in a mechanically ventilated enclosure using CFD models for different ventilation and leak parameters that were empirically validated with a distributed array of gas measurement points—that is through a hydrogen wide area monitor (HyWAM)[1]. It is now necessary to incorporate the hydrogen dispersion behaviour into quantitative risk analysis (QRA) tools, such as HyRAM [10], to quantify risk reductions that can be achieved through an active monitoring system properly integrated into a facility design. This would lead to an optimally deployed gas detection system, resulting in improved facility safety and utilization of physical space. The activity described in this paper focuses on GH_2 releases in enclosed (indoor) facilities, although this strategy is germane to outdoor facilities and LH_2 operations. The development of active monitoring using HyWAM for outdoor LH2 operations is described in a separate paper to be presented at the 2019 ICHS [11]. Thus, sensors play a dual role in hydrogen safety. In addition to validating the fundamental behaviour of released hydrogen dispersion, sensors (or other detection methods) will continue to be used for active monitoring.

The most direct approach for the detection of either planned or unintended hydrogen releases is with sensors, which are electronic devices that generate an easily measured electrical signal or a change in electrical signal (e.g., resistance, voltage, current, frequency) that can be quantitatively related to hydrogen concentration changes in the surrounding environment. Overviews of various hydrogen sensor platform types have recently been published [12−14]. Although slightly different categorizations have been developed to classify hydrogen sensors, the main currently available commercial hydrogen sensor platforms include catalytic sensors (e.g. Ref. [15]), metal oxide sensors (e.g. Ref. [16−18]), electrochemical sensors (e.g. Refs. [19−21]), thermoconductivity sensors (e.g. Ref. [23]), semiconducting platforms (e.g. Ref. [22,23]), optical sensors (e.g. Ref. [24−26]) and sensors based on palladium or palladium alloys coatings (e.g. Ref. [27,28]). Each platform is based upon a unique transduction mechanism that exploits a specific property of hydrogen (e.g., combustibility, electrochemical reactivity, thermo-conductivity, selective adsorption into palladium) to induce a change in an electrical parameter, and each has advantages and limitations. The development of new sensors with improved metrological performance remains an active area of research; critical parameters of interest include selectivity, robustness (e.g. sensor lifetime and stability) and response time, along with lower power requirements and physical miniaturization of the sensing element. Much of the recent activity has been on configuration of the sensor for fast response times through miniaturization strategies the include both advance micro-fabrication methods (e.g. Ref. [28,29]) and nanotechnologies (e.g. Ref. [23,30]). Advanced standoff

[1] Hydrogen Wide Area Monitoring (HyWAM) can be defined as the quantitative spatial and temporal 3-dimensional profiling of either planned or unintended hydrogen releases.

Please cite this article as: Tchouvelev AV et al., Development of risk mitigation guidance for sensor placement inside mechanically ventilated enclosures − Phase 1, International Journal of Hydrogen Energy, https://doi.org/10.1016/j.ijhydene.2020.09.108

detection methods are being explored for hydrogen monitoring, such as LIDAR [31] and Schlieren [32], but such stand-off methods are not commonly available as commercial units, nor can they be easily applied for the quantitative detection of helium, which is often used as a hydrogen surrogate.

Philosophy of approach

The behaviour of released hydrogen is incompletely characterized and often misunderstood, leading to potentially disastrous consequences. For example, one perception held by some hydrogen safety experts was the view that buoyancy would dominate the dispersion of hydrogen releases to preclude potentially hazardous levels of hydrogen more than a few meters below the release point, including the dispersion of cold hydrogen plumes formed during venting of liquid hydrogen (LH_2) storage tanks. This is not the case, and vol% levels of hydrogen will often be observed several meters below the LH_2 release point. In fact, low vol% levels of hydrogen were actually observed nearly 10 m below the point of release during a recent field deployment of the NREL HyWAM [33]. Factors that might influence this dispersion behaviour (such as wind speed and direction, ambient temperature, release rate and direction, etc.) have not been fully elucidated and this is an active area of research (e.g. Refs. [11,34,35]). Gas detection is necessary to elucidate gas dispersion behaviour for both indoor and outdoor applications. Accordingly, the use of hydrogen detection (sensors) to assure facility safety is evolving as is the corresponding hydrogen sensor RD&D needs. For many years sensors have typically been used to assure compliance to code requirements and to meet customer needs as per SIL requirements. Thus, sensor RD&D needs tended to focus on the metrological performance of the sensors [36]. Accordingly, the NREL sensor laboratory focused on sensor performance evaluations. Detection technology is now being used to elucidate hydrogen behaviour to validate CFD models on hydrogen dispersion, which is then to be incorporated into quantitative risk analysis to guide facility design and operations, including optimal sensor placement for highest assurance of safety. Accordingly, the role of the NREL Sensor laboratory is evolving, as illustrated in Fig. 1, which was extracted from the presentation at the HySafe RPW.

The key technical requirement and challenge here is to determine an optimal location for the placement of a hydrogen sensor (or sensors) so that the probability of detection is the highest and independent on the leak orientation/direction. This requires an ability to predict air circulation inside the enclosure depending on location of air intake and exhaust, equipment placement inside the enclosure and air flow generated by the exhaust fan. The key in this regard is to find/predict locations of low ventilation flow within the facility, which assures higher predictability of detection of low hydrogen concentrations, which are undetectable by other means (e.g., pressure sensors mounted on pneumatic lines). From this perspective, spots with hydrogen concentrations between 1000 and 5000 ppm are the primary targets. This is a radically different approach from the current practice targeting hydrogen detection within a range between 8000 and 16,000 ppm.

Adequate prediction of hydrogen concentrations distribution requires an understanding of hydrogen behaviour within the deployment environment, which in turn requires the development of validated models. To address this issue, a study of a real-world mechanically ventilated enclosure containing GH_2 equipment was conducted, where CFD modeling of the hydrogen dispersion (performed by AVT and UQTR – pre- and post-modeling, and independently by the JRC – post-modeling) was validated by the NREL Sensor laboratory using a Hydrogen Wide Area Monitor (HyWAM).

It is important to underscore here that the objective of the study was not to achieve exact matching of experimental results vs CFD modeling, but to obtain agreement on identification of areas with the targeted concentration range within the enclosure.

Pre-modeling

Enclosure geometry and ventilation description

Enclosed electrolytic hydrogen generator at NREL Wind Site containing two electrolyser modules and a hydrogen compressor was selected as a typical packaged enclosure. The detailed measurements of the internal enclosure layout are presented on Fig. 2 below.

CFD modeling domain

The enclosure geometry was reproduced in the CFD modeling domain as shown on Fig. 3 below. The windows and door on the North wall are considered fully sealed and are not taken into account in the modeling. (Note: it was confirmed during the flow measurements that the windows and door are sealed reasonably well).

Ventilation airflow measurements

To verify the airflow of the enclosure exhaust fan, the decision was made to conduct the actual airflow measurements using Air Data Multimeter shown on Fig. 4 below.

The flow measurements determined that the flow through the bottom air inlet and through the exhaust fan turned out to be almost identical and fluctuated around 0.13 m^3/s or 300 cfm. This number was fixed for the purpose of CFD simulations.

Selection of H_2 leak effective diameter and pressure

Selecting a representative leak hole size and thus a representative leak rate has always been a tricky endeavour in hydrogen release modeling. Until recently, published guidances on this matter (like, for example, TNO Purple Book) referred to the oil and gas industry experience, which inevitably led to over conservative approach when applied to significantly smaller hydrogen installations. From this perspective, modeling to determine hazardous areas is likely the best reference for the objectives of this study.

The recent edition of IEC 60079-10–1:2015 [37] provides suggested hole cross sections for secondary grade releases. Of

Please cite this article as: Tchouvelev AV et al., Development of risk mitigation guidance for sensor placement inside mechanically ventilated enclosures – Phase 1, International Journal of Hydrogen Energy, https://doi.org/10.1016/j.ijhydene.2020.09.108

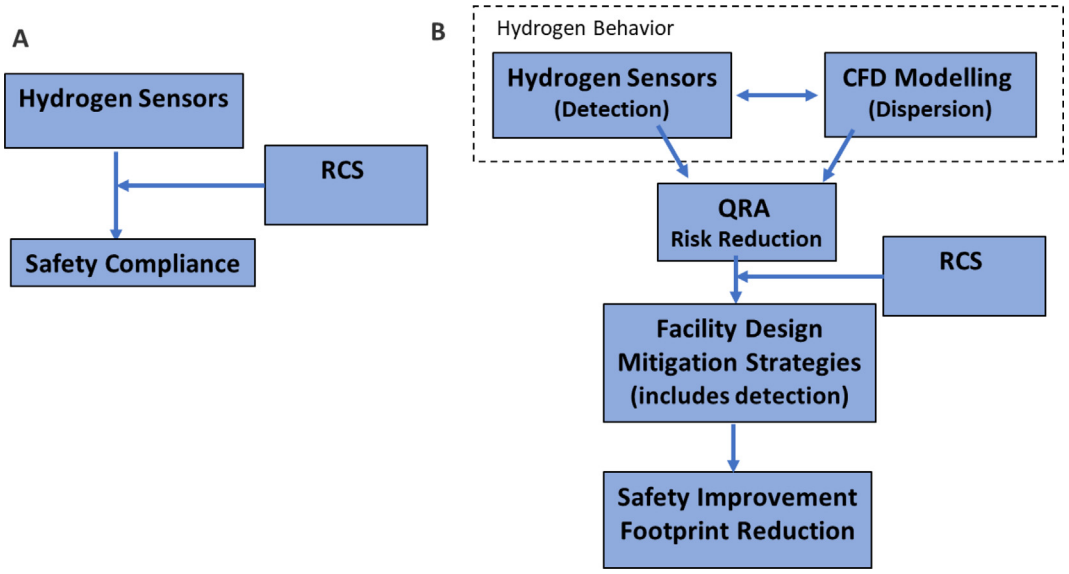

Fig. 1 – (A) H_2 sensors are used as part of a facility safety system to achieve an appropriate SIL while at the same time can assure compliance to prescriptive code requirements. (B) Detection is also needed to verify released hydrogen behaviour (e.g., using HyWAM) to validate dispersion models, and for a facility active monitoring system. Coupled with other mitigation strategies, active monitoring can assure improved safety in smaller footprints (Extracted from summary report from the HySafe RPW [5]).

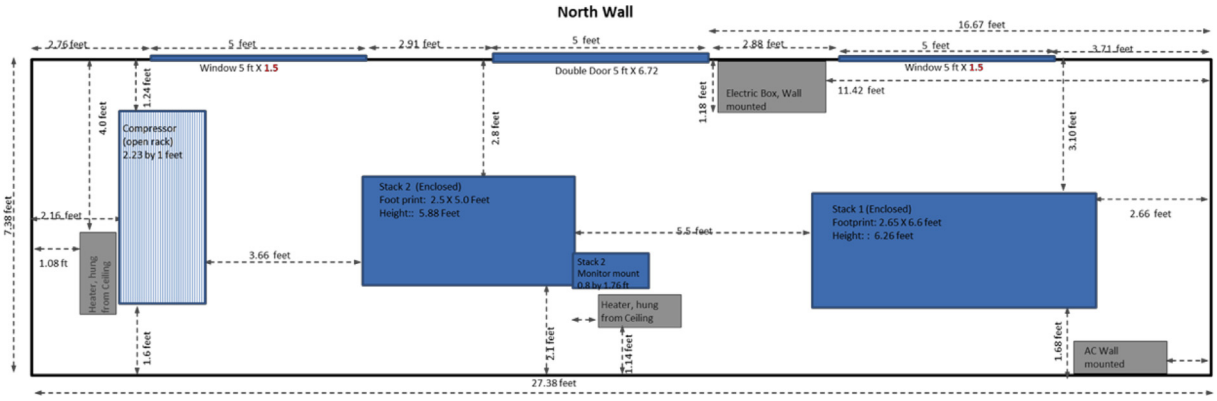

Fig. 2 – General floor plan of the NREL ISO Container (H2 production Unit). Stack 1, Stack 2, and the Compressor are floor mounted. On Stack 2 is a side-mounted Display. The windows and door are on the North Wall. The AC unit sticks out from the South Wall. Two heaters/blowers are mounted from the ceiling. Inside dimensions for the container are given.

particular interest is the suggestion for small pipes and fittings up to 50 mm in diameter. The suggested size of the hole of 0.025 mm^2 translates into **0.18 mm ID**.

The above approach was compared with the recent industry practice as well as advanced approach to hydrogen leak rate data analysis developed by Sandia National Labs (SNL) for the development of NFPA 55 and NFPA 2 standards, which was later incorporated in to ISO/TC 197 work on safety distances. Such analysis of credible references [28–43] concluded that leak sizes between 0.1 and 0.2 mm ID are considered most reasonable to occur (over 95% of all leaks). Thus, the leak orifice of 0.18 mm seems reasonably conservative and representative for the purpose of this study.

Based on actual specifications of the equipment inside the NREL container, the operating and thus leak gauge pressure was set at 0.83 MPa (or 0.93 MPa absolute).

Hydrogen leak location and parameters

The compression fitting on the hydrogen line from the PEM electrolyser unit to the compressor located between two electrolyser units on the South wall was selected as the leak

Please cite this article as: Tchouvelev AV et al., Development of risk mitigation guidance for sensor placement inside mechanically ventilated enclosures – Phase 1, International Journal of Hydrogen Energy, https://doi.org/10.1016/j.ijhydene.2020.09.108

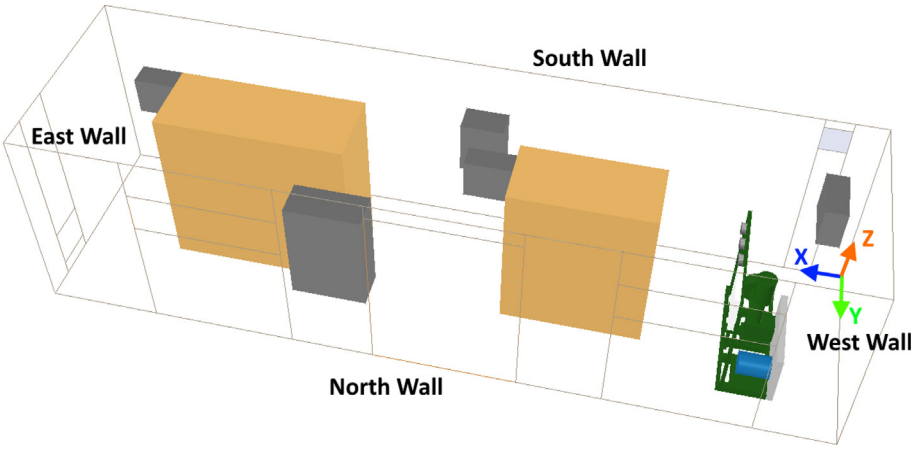

Fig. 3 – NREL container as modelled in PHOENICS.

Fig. 4 – Vent flow measurement system used to measure the actual flow through vent inlet and the exhaust fan.

origin as shown on Fig. 5. Hydrogen leak was modelled in 3 directions: horizontal towards N wall, horizontal towards E wall and vertical. Horizontal N wall case was chosen for comparison with Helium for the planed tests at NREL.

Hydrogen leak parameters for CFD simulations are summarized in Table 1 below.

Simulation results

Table 2 shows the comparison of the cloud contour at 2.5% LFL (0.1% molar fraction), 5% LFL (0.2% molar fraction) and 10% LFL (0.4% molar fraction) 540 s after the onset of the leak for various leak orientations. The molar fraction is also shown at the probe "pencil" location which is set at x = 4.1 m, y = 1.7 m and z = 2.2 m, which corresponds to the region below the enclosure ceiling where hydrogen is most likely to be found following the release and dispersion from the selected leak location on the South wall between stack 1 and 2 regardless of its orientation.

The images in Table 2 indicate that in the context of this project, concentrations above 5% LFL may not be practically relevant. The key objective of the project is to find a concentration distribution (dispersion) pattern that would pinpoint a spot where H_2 can be detected regardless of the leak direction. From this perspective, concentrations above 5% LFL appear to be too high for this enclosure configuration as demonstrated by the images in the right column. These plumes considered alone provide no clue on how to achieve the project objective. It appears that the optimum and practical concentration level is somewhere between 1000 and 2000 ppm or 2.5% and 5% LFL. At these levels one can have a reliable and early warning that a leak is present inside an enclosure.

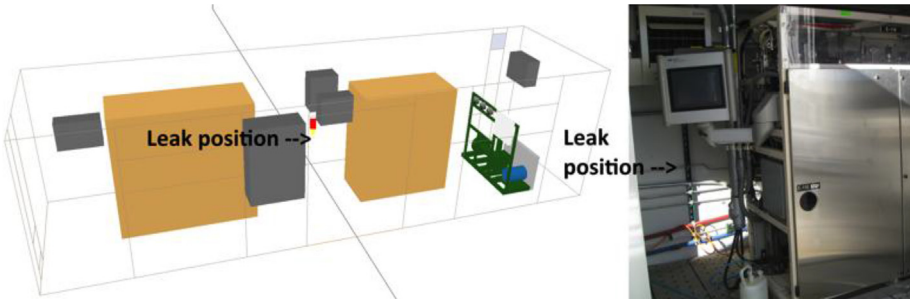

Fig. 5 – Leak position in the simulation domain (left) and the corresponding compression fitting location on the South wall of the NREL container (right).

Please cite this article as: Tchouvelev AV et al., Development of risk mitigation guidance for sensor placement inside mechanically ventilated enclosures – Phase 1, International Journal of Hydrogen Energy, https://doi.org/10.1016/j.ijhydene.2020.09.108

Table 1 – Hydrogen leak parameters.

Leak position (origin: lower corner of the South and West walls)	X = 4 m, Y = 0.05 m, Z = 0.6 m
Leak diameter	0.18 mm
Storage pressure (gauge)	0.83 MPa
Effective diameter (Birch et al., 1984)	0.41 mm
Effective exit density (Birch et al., 1984)	0.0838 kg/m^3
Mass flow rate (remains constant)	1.4752 10 ^{5} kg/s
Temperature (remains constant)	293.15 K
Ambient pressure	101,325 Pa
Turbulence Intensity	5%
Average mesh size	600,000 elements

Helium leak modeling

Helium leak is modelled for the specific purpose of supporting planned helium release experiments inside the container at NREL Wind Site. For safety reasons, NREL made a decision to use helium as a test medium to represent H_2 behaviour. From this perspective, it is important to ensure that He release setup is scaled appropriately to adequately represent hydrogen taking into account differences in their physical properties.

US DOE has used He in validation experiments as an alternative for hydrogen before [44]. Helium has also been recognized as an appropriate hydrogen surrogate in the United Nations Global Technical Regulation 13 (GTR 13) [45], which provides the basis for internationally harmonized regulations on light-duty hydrogen vehicle safety. GTR-13 allows vehicle on-board storage tanks to be pressurized with either hydrogen or helium during vehicle crash tests; following the crash test the integrity of the fuel system must be maintained such that hydrogen/helium will not be present within vehicle compartments. The NREL sensor laboratory identified and demonstrated a commercial thermoconductivity sensor that would not only survive vehicle crash tests but could detect either hydrogen and helium [46,47]. Unlike other common sensor platforms which will not respond to helium, the thermo-conductivity sensor is highly sensitive to both hydrogen and helium, and this makes it an ideal sensor for modeling studies that use helium as a hydrogen surrogate. The TC sensor also has a fast response time relative to many other commercial platforms, with a t_{90} that can be less than 1 s [48]. Accordingly, a thermoconductivity sensor was selected for the NREL HyWAM deployed in this investigation and was the sensor used in earlier HyWAM deployments for cold hydrogen plumes [49].

However, helium and hydrogen differ in their thermodynamic and hydrodynamic properties, such as buoyancy, turbulence, diffusion and density, as was shown earlier in the similarity theory analysis [50]. Richardson number is the most sensitive to scaling – its distortion is 53% moving from He to H_2. Hence, adjusting the Richardson number appropriately ensures a good agreement between hydrogen and scaled helium leaks.

A close up on the Richardson number scaling with the focus on specifically well-defined plumes of 5% and 10% LFL is shown on Fig. 6 below. In close view the images in both columns look very similar. What is of particular importance is that the probe registers almost identical mole fractions.

Table 2 – Cloud contour at 2.5% LFL, 5% LFL and 10% LFL, 540 s after the onset of the leak for a horizontal release directed toward the North wall, horizontal release directed toward the East wall and vertical release directed toward the ceiling. Mole fraction and corresponding LFL values at the probe location (x = 4.1 m, y = 1.7 m and z = 2.2 m) are also provided.

	2.5% LFL	5% LFL	10% LFL
Horizontal N-wall Probe: 0.11% mole fraction (2.75% LFL)	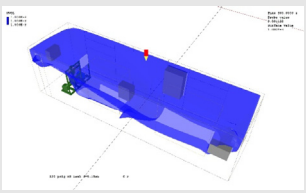	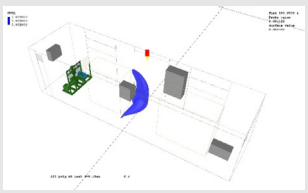	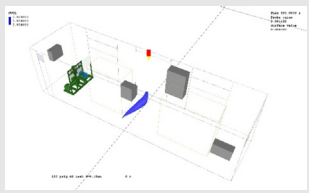
Horizontal E-wall Probe: 0.25% mole fraction (6.25% LFL)	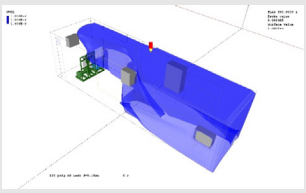	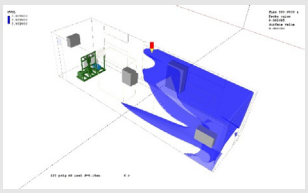	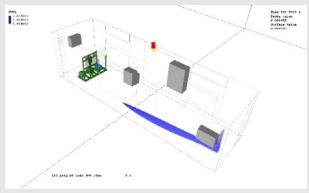
Ver cal Probe: 0.43% mole fraction (10.75% LFL)	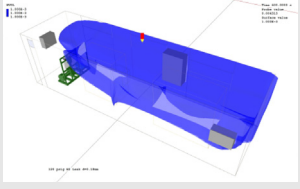	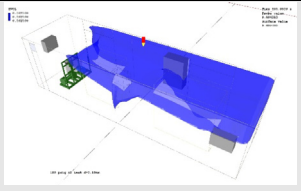	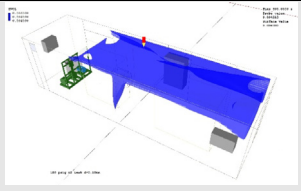

Please cite this article as: Tchouvelev AV et al., Development of risk mitigation guidance for sensor placement inside mechanically ventilated enclosures – Phase 1, International Journal of Hydrogen Energy, https://doi.org/10.1016/j.ijhydene.2020.09.108

Helium experiments set UP and results

As noted above, the focus of this study was on indoor hydrogen dispersions within a representative *small* facility or enclosure. Helium was chosen as a surrogate for hydrogen for release tests. The release parameters as well as the point of leak location were guided by the analysis described in the previous section (3.0) of this paper. Various leak orientations were considered (up/down, horizontal N and E). The "standard" release condition was such that the release was orientated "up". For this study, a 10-sensor hydrogen HyWAM module was deployed within a mechanically ventilated ISO container that housed two electrolyzer units and a compressor as explained in Section Enclosure geometry and ventilation description and illustrated on Figs. 2 and 3. The electrolyzers were used to produce hydrogen for the NREL Hydrogen Dispenser formerly deployed within the NREL Wind Technology Center [51]. The ISO container served as a model system for investigating the impact of active ventilation on hydrogen dispersion within an indoor facility.

The NREL HyWAM module consisted of 10 commercial thermo-conductivity (TC) hydrogen sensors (Xensor Integration, BV, Model XEN-5320-USB) and 8 K-type thermocouples (Omega) for in-situ temperature measurements [33]. The TC sensor has a response time (t_{90}) of 250 ms, allowing for the quantitative measurements of fast hydrogen transients. This hydrogen sensor has a broad measuring range up to 100 vol% H_2. Although designed primarily for hydrogen, the TC sensor is also sensitive to helium such that the vol% He can be obtained through a simple empirical calibration expression:

$$\text{vol\% He} = 0.7*(\text{vol\% H}_2)_{\text{equivalent}}$$

where $(\text{vol\% H}_2)_{\text{equivalent}}$ is the observed sensor output signal induced by the helium-containing test gas. The timing of the gas release was controlled through a pneumatic valve that was remotely and manually operated activated, with a typical release time of 10 min. A typical measurement thus consisted of a 5-min baseline prior to the release, a 10-min release during which time the pneumatic valve was opened, and a 20-min recover step to allow the facility to be purged of helium as indicated by a return to baseline of the TC sensor. Typically, this cycle was performed 2 times.

Ten gas sample lines were positioned within the enclosure (see Table 3 and Fig. 7, referenced to the orientation of Fig. 8) to draw gas from precise locations within the enclosure to the remotely deployed HyWAM modules. Gas samples were continuously delivered to each TC sensor (purge time < 1sec) through the use of a sample pump.

(Chamber: X = 8.35m, Y = 2.24m, Z = 2.2 m).

Filled circles indicate helium and temperature measurements. Shaded circles imply multiple sampling points with same X,Y coordinates but different Z (vertical) value. Open circles indicate helium measurements only. Release Point Coordinates: X = 4.0 m, Y = 0.05 m, Z = 0.6 m. The release orientations were up (toward ceiling) and horizontal (E, W, and S).

Fig. 8 shows representative measurements during the "standard" UP release conditions.

Table 3 – Release and monitoring positions for the indoor helium release measurements.

		Sample Point (SP) Position				
	Release Point	SP 1	SP 2	SP 3	SP 4	SP 5
X	4.0	8.0	8.0	6.62	2.8	0.4
Y	0.05	1.3	1.3	1.87	1.7	0.4
Z	0.60	2.2	0.3	2.20	2.2	0.4
		Sample Point (SP) Position				
	"Pencil Point"	SP 6	SP 7	SP 8	SP 9	SP10
X	4.1	0.4	4.1	4.8	4.6	1.8
Y	1.7	0.4	1.7	1.7	1.7	0.4
Z	2.2	2.1	2.2	2.1	2.2	2.1

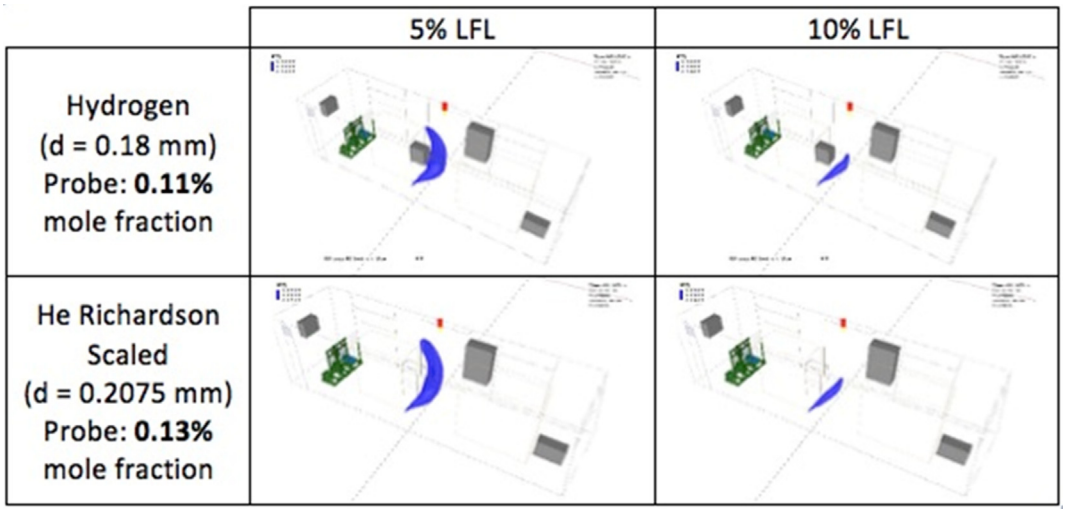

Fig. 6 – Close up of 5% and 10% LFL iso-contours for hydrogen and helium scaled to match the Richardson number.

Please cite this article as: Tchouvelev AV et al., Development of risk mitigation guidance for sensor placement inside mechanically ventilated enclosures – Phase 1, International Journal of Hydrogen Energy, https://doi.org/10.1016/j.ijhydene.2020.09.108

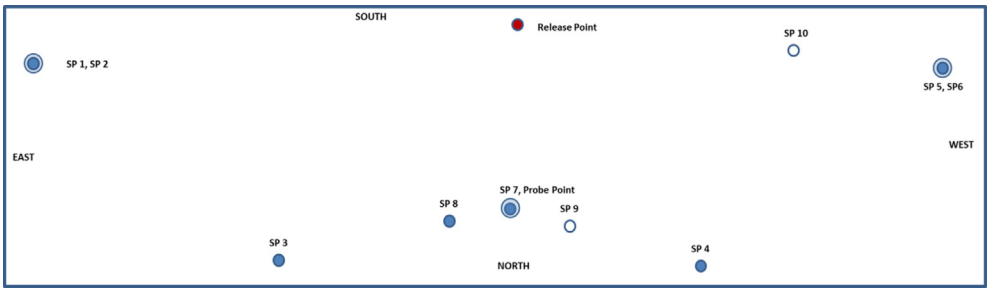

Fig. 7 – Location of He sensors for release tests – plan view: X (North, South) – Y (East, West) plane; coordinates origin – top right corner.

Helium post-modeling results

JRC CFD modeling – (or CFD simulations of a 10 min vertical release)

In the selected experiment, the helium was released for 10 min, the pressure in the release pipe was 0.83 MPa gauge or 0.93 MPa absolute, and the mass flow rate was 0.0360 g/s. Modeling the real orifice (nozzle) is very demanding from the computational point of view in terms of mesh resolution and computer run-time. To reduce the expensive computational demands, the actual nozzle was replaced by a notional nozzle, which has a larger area but with the same flow rate as the real one and at ambient pressure and uniform velocity [52]. The real nozzle diameter is 0.178 mm while the notional nozzle diameter is 0.519 mm. The ideal gas law was used in the Birch model and in the simulations. Since the absolute pressure in the release pipe is 0.93 MPa in the selected experiment, the inaccuracy due to the ideal gas law compared to a real gas equation is negligible.

Isothermal conditions were assumed for the simulations with the ANSYS CFX 16.0 code. The simulations were performed in 3 stages: a first stage without gas release to capture only the velocity field due to the ventilation, a second stage with the helium release and the ventilation, and a final stage after the release is finished with only the ventilation. On the left hand side of Fig. 9, the computational model is illustrated while on the right hand side, the complex flow field generated by the mechanical ventilation before the beginning of the helium release is shown.

The computational mesh is about 0.8 million nodes. The turbulence model is the SST Transitional (Gamma Theta) model which is the recommended transition model for general-purpose applications. The k-ω based Shear-Stress-Transport (SST) model was originally developed to better include transport effects into the formulation of the eddy-viscosity [53]. The full transition model is based on two transport equations, one for the intermittency and one for the transition onset criteria in terms of momentum thickness Reynolds number. It uses an empirical correlation [54], which has been developed to cover standard bypass transition as well as flows in low free-stream turbulence environments and it has been extensively validated with the SST turbulence model for a wide range of transitional flows. In Fig. 10, a snapshot of the concentration field at 10 s before the end of the release is shown.

The position of the sensors for the concentration measurements is illustrated in Fig. 11. As shown in Fig. 12, from the qualitative point of view, the behaviour in the experiment is well reproduced in the simulation for all sensors: the concentration grows and decreases with a very similar timing in the experiment and in the simulation. Only in few sensors, e.g. SP3 and SP4, the arrival of the helium is anticipated in the simulation compared to the experiment. From the quantitative point of view, the agreement between experimental data and simulation results for the concentration can be considered satisfactory for some sensors (SP2, SP5, SP6, SP7, and SP10) while for other sensors, the concentration is underestimated in the simulation. Nevertheless, overall the simulation accuracy is considered to be sufficient for the purpose of this investigation.

The results shown on Fig. 12 above are consistent with the summary of experimental and modeling results shown on Fig. 15 below for criteria 1b and 1c listed in Section Phase 1 results summary and recommendations.

AVT/UQTR modeling

A sample of air circulation inside the enclosure during the tests is shown on Fig. 13.

Virtual sensors – sample points locations inside the CFD modeling domain for the He tests are shown on Fig. 14 below. Those correspond actual H2 sensors locations shown on Fig. 7.

Comparison of simulation results with test data

The comparison of simulation results with He release test data was arranged in sets of 4 graphs for each sensor (SP) location. The first pair of graphs showed the experimental and simulation results for a horizontal helium release directed towards the North wall for the experiments done in September 2017 and December 2017. The second pair showed the comparison graphs for a horizontal helium release directed towards the East wall as well as for an Upward helium release directed towards the ceiling. As mentioned above, some of the sensor coordinates changed from September to December tests. This allowed for the sensitivity analysis in regards to sensor locations.

Please cite this article as: Tchouvelev AV et al., Development of risk mitigation guidance for sensor placement inside mechanically ventilated enclosures – Phase 1, International Journal of Hydrogen Energy, https://doi.org/10.1016/j.ijhydene.2020.09.108

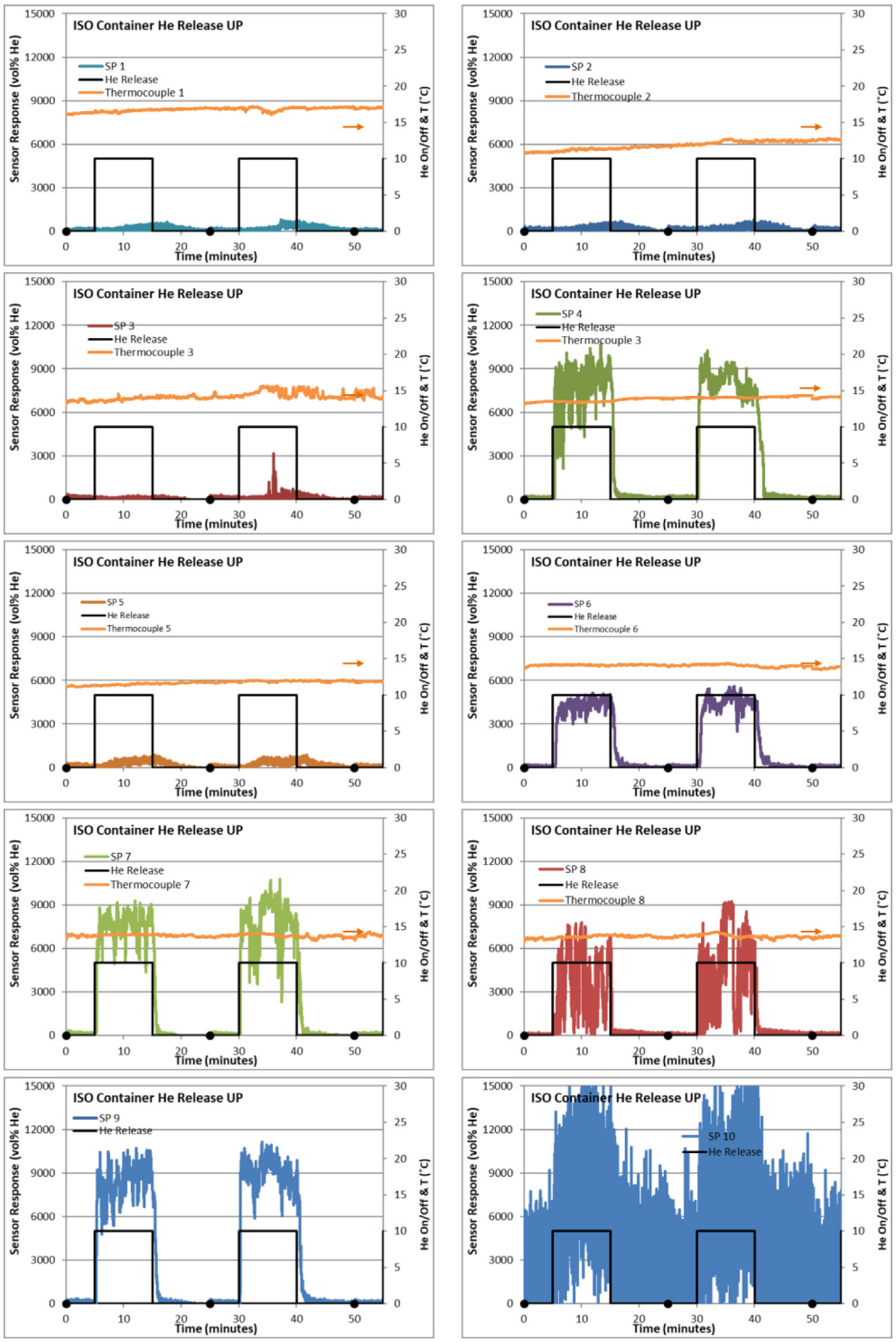

Fig. 8 – Sample of He measurements for UP release conditions. Y axis units for Sensor Response are ppmv He.

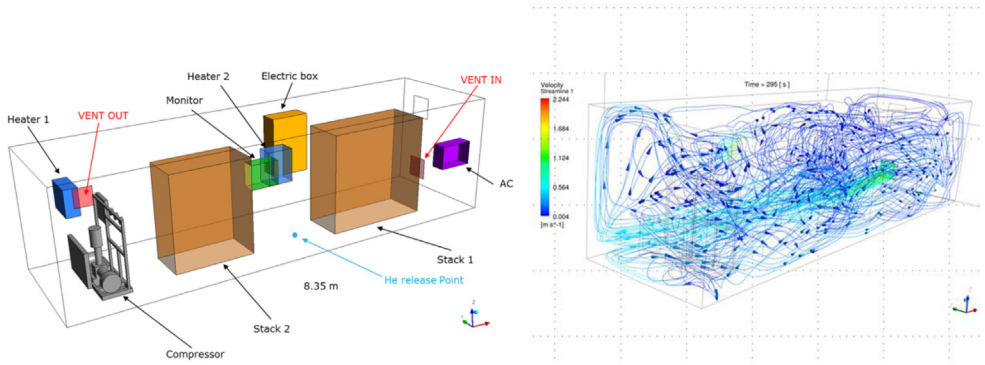

Fig. 9 – On the left hand-side: computational model of the facility, including the vents and the position of the gas release. On the right hand side: snapshot of the velocity field before the beginning of the helium release.

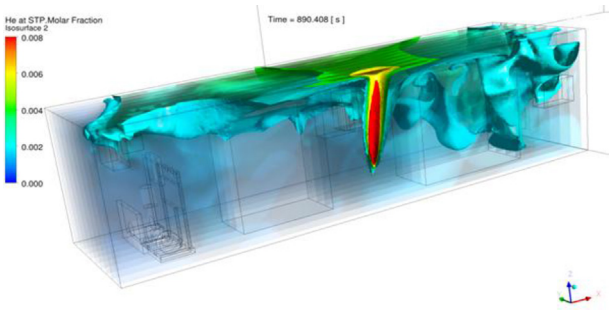

Fig. 10 – Helium molar fraction at 10 s before the end of the release.

During the comparison of the experimental results for North releases for SPs 4, 6, 7, 8, 9 and 10, a significant (between 50 and 100% in real values) concentration increase in December tests vs September tests was noticed. Two potential explanations were proposed:

1 The proximity of the monitor points to the enclosure ceiling. In September tests the monitor points were set a bit lower from the ceiling compared to the December tests.
   a Ceiling piping could trap some of the gas there and restrict air movement thus leading to spatial He concentration increase.
   b The other contributing factor is that closer to the ceiling (and any surface for that matter) air velocity naturally decreases.
   c Hence, the combination of these two factors: extra obstacles restring air movement and lower air velocity closer to the ceiling, may explain why the results from September tests when sensors were positioned bellow the piping and farther from the ceiling yielded lower overall concentration measurements. That is why September test measurements were closer to the simulations with active ventilation (300 cfm).
2 The active airflow inside the container was indeed somewhat different in September vs December tests. This is a reasonable proposition considering that weather conditions at the NREL Wind Test Site (affecting wind direction and temperature) may randomly change during the day. This could certainty influence air intake and exhaust rates inside the container thus affecting the most sensitive spots inside the container around SPs 7, 8 and 9.

For this reason, the post-modeling focused on testing the sensitivity of He concentrations depending on the airflow inside the enclosure. In this regard, four airflow regimes were compared: no mechanical ventilation, quarter-ventilation flow (75 cfm), half-ventilation flow (150 cfm) and full ventilation flow (300 cfm).

Monitor points close to the release point (7, 8 and 9) see much higher concentration in the experiment than in the

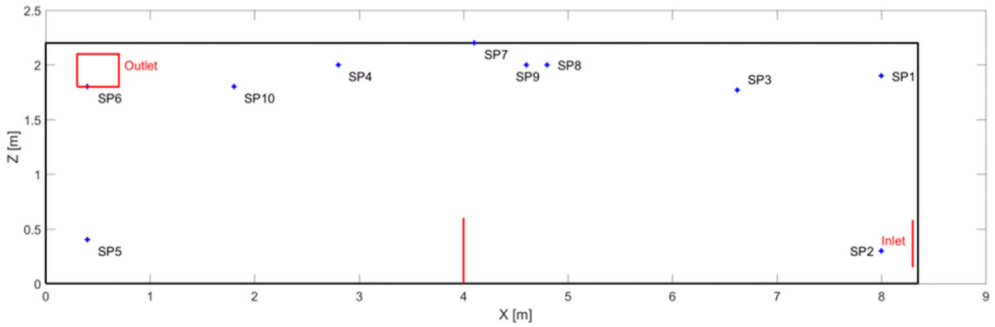

Fig. 11 – Position of the sensors (SP) for the measurements of helium concentration in a vertical plane.

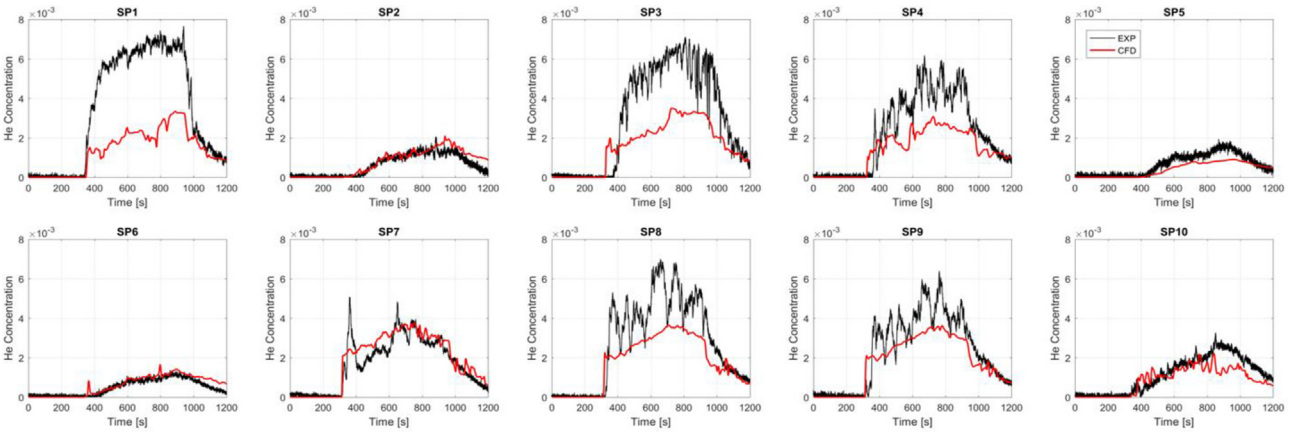

Fig. 12 – Comparison between experimental data (black) and simulation results (red) for the helium concentration. (For interpretation of the references to color in this figure legend, the reader is referred to the Web version of this article.)

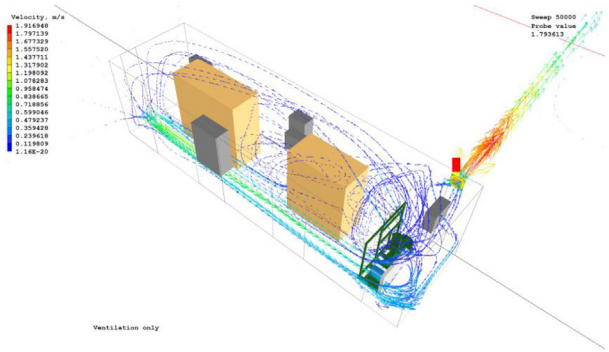

Fig. 13 – Steady state air circulation profile at 300 cfm as modelled in PHOENICS.

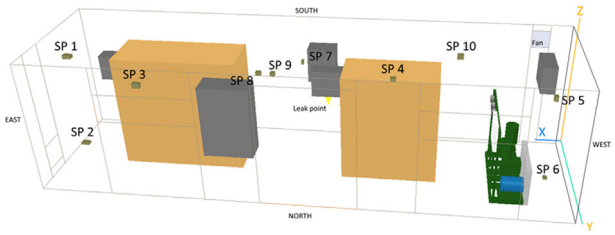

Fig. 14 – Virtual sample point positions inside the CFD domain for release tests performed at NREL in September 2017. Release tests in December 2017 had some sensors moved along vertical direction to test sensitivity.

simulation with a higher ventilation rate. On the other hand, the monitor points on the floor and away from the vent exit show greater agreement with the experiment when higher ventilation rates are considered.

Making an assumption that airflow in the test container during the tests in September 2017 in the North wall direction was the closest to the CFD simulation setting, let us base our preliminary recommendations for sensor placement strategy on the test and CFD simulation results presented below on Fig. 15.

Phase 1 results summary and recommendations

Preliminary recommendations for sensor placement strategies inside a ventilated enclosure are presented on Fig. 16 below. Those are based on the following observations arising from reviewing the graphs on Fig. 15:

1. SP10 graph shows the widest gap between two lowest dashed lines corresponding to 300 and 150 cfm airflow respectively. This indicates that SP10 location is the most sensitive to airflow inside the enclosure. Also, the lowest He concentration corresponding to 300 cfm is too low to be practical – less than a 1000 ppm.
2. SP1, SP3, SP7 and SP8 graphs show a bit narrower gap between 300 and 150 cfm predictions. Also, their lowest readings are above 1000 ppm, which should be viewed as the lowest boundary for practical applications.
3. Locations SP2, SP5 and SP6 have the least sensitivity to airflow, however, their readings are on the border line of practicality (1000 ppm) and thus may not be very useful for practical applications.
   a Note: In December tests, SP6 was moved close to the exhaust fan. As the test data showed this location showed high sensitivity to airflow. This confirms that placing a sensor close to an exhaust fan is not a suitable location. This explains why there is a red arrow pointing at SP6 in the bottom image on Fig. 16.

Based on the above observations, the following recommendations seem reasonable subject to further analysis and confirmation:

1. Suitable locations for sensor placement in a ventilated enclosure are those that meet the following criteria:
   a Not on a direct path of the airflow from the air inlet to the exhaust fan. This ensures weak to moderate sensitivity to potentially fluctuating airflow;

Please cite this article as: Tchouvelev AV et al., Development of risk mitigation guidance for sensor placement inside mechanically ventilated enclosures – Phase 1, International Journal of Hydrogen Energy, https://doi.org/10.1016/j.ijhydene.2020.09.108

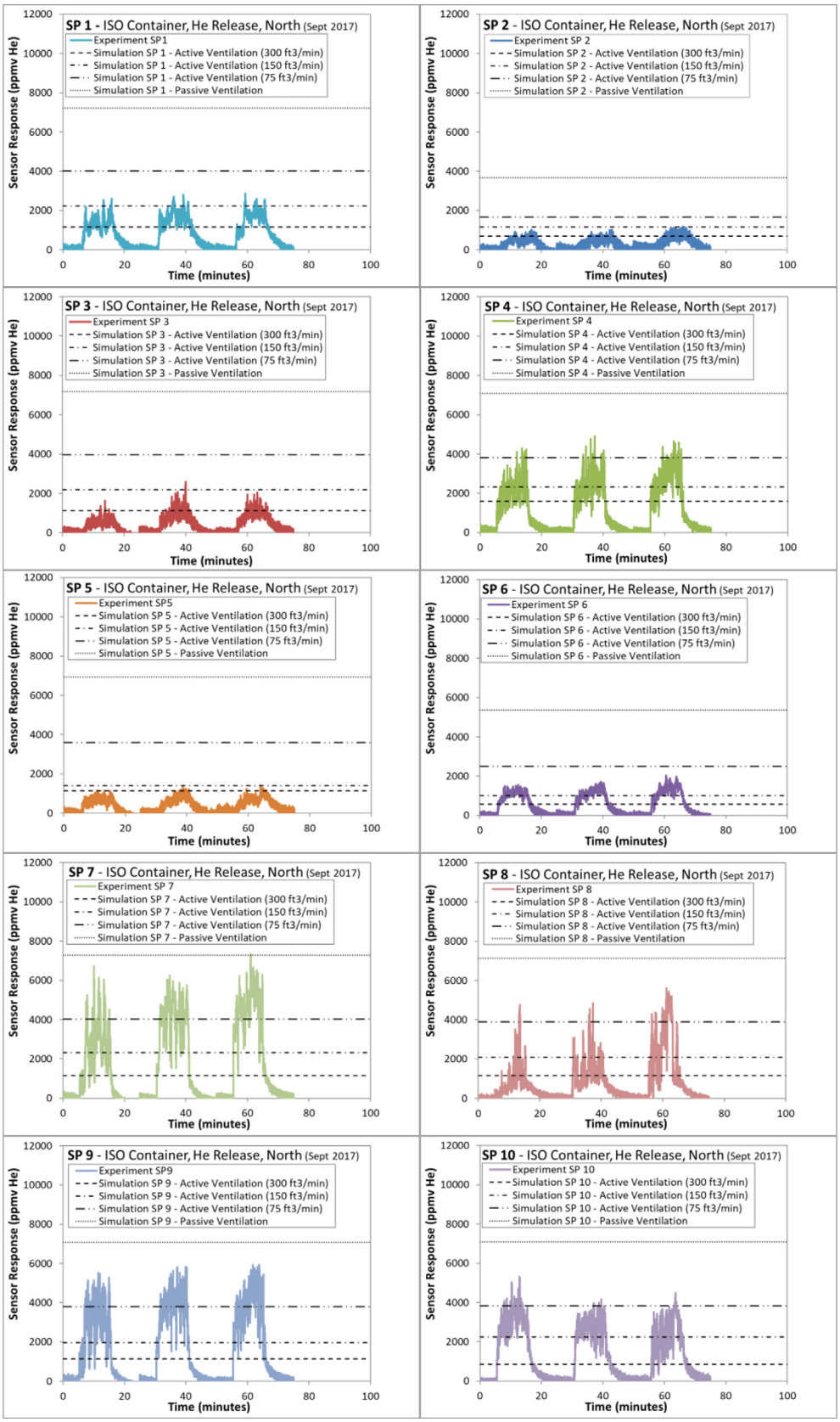

Fig. 15 – Test hydrogen sensor responses (2017-09-28) for each of the 10 sampling points compared with simulation results for the same sampling points. The orientation of the leak was horizontal towards the North wall. Horizontal dashed lines show CFD predicted He concentrations for different airflows.

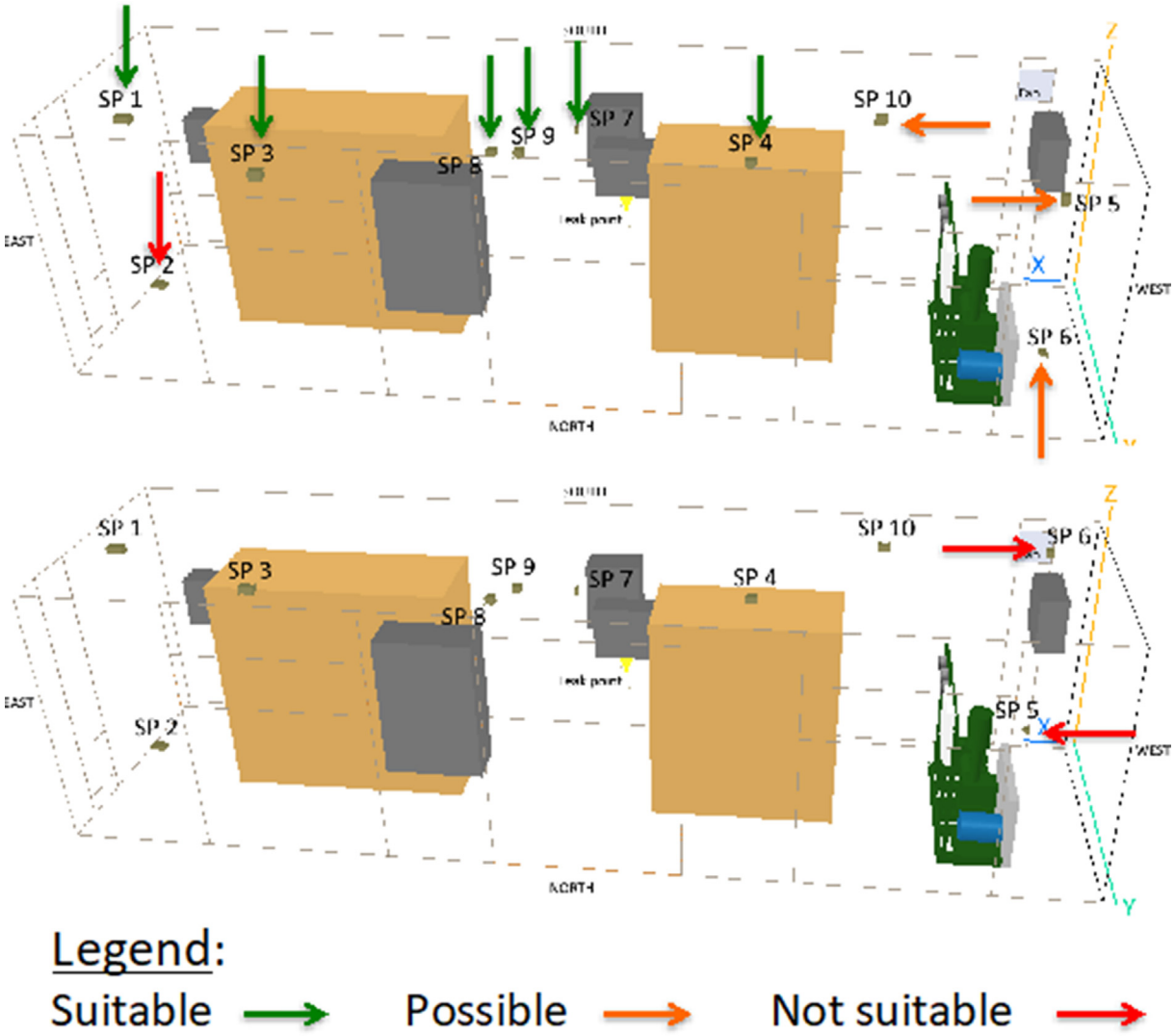

Fig. 16 – Preliminary recommendations for sensor placement strategy. Top shows September sensor setting, bottom – December setting.

b Minimum expected concentration is above the minimum practical level of 1000 ppm, while the maximum expected concentration is below 10,000 ppm. For this reason, locations close to the floor, although having low sensitivity to airflow, may not be practical since their expected concentration levels are on the borderline of practicality and reliable sensor detection threshold.
c Below the enclosure ceiling thus not obstructed by the ceiling piping and lighting fixtures or other objects. This ensures unobstructed relatively low velocity and low turbulence airflow around the sensor sampling point.

2. Based on the above criteria:
   a Locations SP1, SP3, SP4, SP7, SP8 and SP9 seem suitable options for sensor placement – green arrows;
   b Locations SP10, SP5 and SP6 shown on the top image of Fig. 6 (reflecting North release on Sep 28) don't seem to be optimum, but need to be further investigated as they may work in some cases – orange arrows
   c Location SP2 does not seem to be suitable due to low readings – red arrow.
   d Locations SP 5 and SP 6 on the bottom image (December tests) don't seem to be suitable either due to low readings (SP5) or high sensitivity to airflow (SP6) – red arrows.

It is fair to say that specific sensor locations will depend on the internal configuration of the enclosure, specific leak/accident scenarios and arrangement of mechanical ventilation. However, the basic recommendations stated above should still apply.

More sensitivity analysis is needed to draw more definitive conclusions. Expansion of indoor releases to other larger facilities (including underground parking, vehicle maintenance facilities and tunnels) and incorporation into QRA tools, such as HyRAM (Hydrogen Risk Assessment Models) is planned for Phase 2.

Specifically, Phase 2 will focus on the following scope:

Please cite this article as: Tchouvelev AV et al., Development of risk mitigation guidance for sensor placement inside mechanically ventilated enclosures – Phase 1, International Journal of Hydrogen Energy, https://doi.org/10.1016/j.ijhydene.2020.09.108

Sensitivity analysis of the impact of variations in the test parameters relative to the conditions assumed in the initial phase. The sensitivity analysis shall then be used to determine the robustness of the validated model. A small impact on the hydrogen dispersion induced by a "large" variation in the physical parameter will be an indication of model robustness. In contrast, a large impact on dispersion induced by a relatively small parameter variation will be indicative of the need to control the variation of the parameter so as to minimize impacts and more accurately predict dispersion behaviour.

Facility scaling: An empirically validated CFD model for a "small" indoor hydrogen facility will be expanded to a "large" facility (defined as having a volume that is a minimum of five times larger than the ISO container) Empirical validation will be responsibility of NREL. Specific candidate facilities include a light duty FCEV maintenance facility and a parking structure.

Risk Reduction Credits – Incorporate QRA (plug-in to HyRAM): Active monitoring is one mitigation strategy to lower risks within hydrogen facilities. The magnitude of the risk reduction can be estimated using tools known as quantitative risk analysis. HyRAM is one such tool developed by SNL for use in hydrogen facilities, and is open to public. The CFD dispersion model outcome to guide sensor placement for active monitoring is to be adapted so that it can be plugged-in or incorporated to HyRAM QRA mode and the resulting risk calculated. This approach can be used for estimating risk reduction credits due to active hydrogen monitoring. As the first step of this exercise, a known notional nozzle model (e.g. Birch 1984) will be used to test the feasibility of an external model plug-in (incorporation) to HyRAM.

It is anticipated that results of this work will be used to inform national and international standards such as NFPA 2 Hydrogen Technologies Code, Canadian Hydrogen Installation Code (CHIC) and relevant ISO/TC 197 and CEN documents.

Declaration of competing interest

The authors declare that they have no known competing financial interests or personal relationships that could have appeared to influence the work reported in this paper.

Acknowledgements

This work was authored in part by the National Renewable Energy Laboratory, operated by Alliance for Sustainable Energy, LLC, for the U.S. Department of Energy (DOE) under Contract No. DE-AC36-08GO28308. Funding provided by U.S. Department of Energy Office of Energy Efficiency and Renewable Energy Hydrogen and Fuel Cell Technologies. The views expressed in the article do not necessarily represent the views of the DOE or the U.S. Government. The U.S. Government retains and the publisher, by accepting the article for publication, acknowledges that the U.S. Government retains a nonexclusive, paid-up, irrevocable, worldwide license to publish or reproduce the published form of this work, or allow others to do so, for U.S. Government purposes. This work was also funded by the Joint Research Centre of the European Commission (EC JRC).

REFERENCES

[1] National Fire Protection Association (NFPA) 2. Hydrogen Technologies code. 2016.
[2] Canadian hydrogen installation code, CAN/BNQ 1784-000. 2007.
[3] 2015 International Fire code (IFC). 2015.
[4] ISO 19880-1:2019 Gaseous hydrogen - Fueling stations - Part1: General requirements.
[5] Buttner William J, Tchouvelev Andrei, Gardner Lee, Melideo Daniele. Mitigation, sensors, hazard prevention and risk reduction, section 8 in the 2018 HySafe safety research priority workshop summary report. 2018.
[6] International association for hydrogen safety "Research Priorities Workshop", September 2018. Buxton, UK: Final reprort published by Health and Safety Executive; 2020, ISBN 9780717667055.
[7] Ortiz Cebolla R, Weidner E, Bonato C, Buttner W. Summary report for a hydrogen sensor workshop–hydrogen safety sensors and their use in applications with hydrogen as an alternative fuel Brussels, Belgium. 2017 (see, https://ec.europa.eu/jrc/en/publication/summary-report-hydrogen-sensor-workshop-hydrogen-safety-sensors-and-their-use-applications-hydrogen. " EUR 28852 EN.
[8] Boon-Brett L, Bousek J, Castello P, Salyk O, Harskamp F, Aldea L, Tinaut F. Reliability of commercially available hydrogen sensors for detection of hydrogen at critical concentrations: Part i - testing facility and methodologies. Int J Hydrogen Energy 2008;33(24):7648–57. https://doi.org/10.1016/j.ijhydene.2008.10.004.
[9] Buttner W. NREL sensor testing laboratory, Fuel cells program 2018 annual merit review and peer evaluation. Washington, DC: U.S. Department of Energy Hydrogen and; 2018.
[10] Groth K. Hydrogen quantitative risk assessment. Washington DC: DOE Hydrogen and Fuel Cells Annual Merit Review; 2016.
[11] Buttner William J, Hall Jonathan, Hooker Philip, Simon Coldrick, Wischmeyer Tashi. Hydrogen wide area monitoring of LH2 releases. Adelaide, Australia: ICHS2019; 2019.
[12] Buttner WJ, Post MB, Burgess R, Rivkin C. An overview of hydrogen safety sensors and requirements. Int J Hydrogen Energy 2011;36(3):2462–70. https://doi.org/10.1016/j.ijhydene.2010.04.176.
[13] Hübert T, Boon-Brett L, Black G, Banach U. "Hydrogen sensors – a review. Sensor Actuator B Chem 2011;157(2):329–52. https://doi.org/10.1016/j.snb.2011.04.070.
[14] Hübert T, Boon-Brett L, Buttner W. Sensors for safety and process control in hydrogen Technologies. 2018. https://www.crcpress.com/Sensors-for-Safety-and-Process-Control-in-Hydrogen-Technologies/Hubert-Boon-Brett-Buttner/p/book/9781138894341.
[15] Jones MG, Nevell TG. The detection of hydrogen using catalytic flammable gas sensors. Sensor Actuator B Chem 1989;16(3):215–24.
[16] Ihokura Kousuke, Watson James. The stannic oxide gas sensor–prinicples and applications. " CRC Press; 1994, ISBN 9780849326042.

[17] Shen Y, Wang W, Fan A, Wei D, Liu W, Han C, Shen Y, Meng D, San X. Highly sensitive hydrogen sensors based on SnO2 nanomaterials with different morphologies. Int J Hydrogen Energy 2015;40(45):15773–9. https://doi.org/10.1016/j.ijhydene.2015.09.077.
[18] Li Z, Yao Z, Haidry AA, Plecenik T, Xie L, Sun L, Fatima Q. Resistive-type hydrogen gas sensor based on TiO2: a review. Int J Hydrogen Energy 2018;43(45):21114–32. https://doi.org/10.1016/j.ijhydene.2018.09.051.
[19] Joseph R. Stetter, han san-Do, and Ghenadii Korotchenkov, "review of electrochemical hydrogen sensors. Chem Rev 2009;109(3):1402–33.
[20] Sakthivel M, Weppner W. A portable limiting current solid-state electrochemical diffusion hole type hydrogen sensor device for biomass fuel reactors: engineering aspect. Int J Hydrogen Energy 2008;33(2):905–11. https://doi.org/10.1016/j.ijhydene.2007.10.048.
[21] Carter MT, Stetter JR, Findlay MW, Patel V. Advanced electrochemical gas sensors employing novel designs and electrolytes. Boston, MA: "; 2011.
[22] Luo Y, Zhang C, Zheng B, Geng X, Debliquy M. Hydrogen sensors based on noble metal doped metal-oxide semiconductor: a review. Int J Hydrogen Energy 2017;42(31):20386–97. https://doi.org/10.1016/j.ijhydene.2017.06.066.
[23] Zhong A, Sasaki T, Hane K. Comparative study of Schottky diode type hydrogen sensors based on a honeycomb GaN nanonetwork and on a planar GaN film. Int J Hydrogen Energy 2014;39(16):8564–75. https://doi.org/10.1016/j.ijhydene.2014.03.120.
[24] Wang H, Gao G, Wu G, Zhao H, Qi W, Chen K, Zhang W, Li Y. Fast hydrogen diffusion induced by hydrogen pre-split for gasochromic based optical hydrogen sensors. Int J Hydrogen Energy 2019;44(29):15665–76. https://doi.org/10.1016/j.ijhydene.2019.04.026.
[25] Zhang Y, Peng H, Qian X, Zhang Y, An G, Zhao Y. Recent advancements in optical fiber hydrogen sensors. Sensor Actuator B Chem 2017;244:393–416. https://doi.org/10.1016/j.snb.2017.01.004.
[26] Aleixandre M, Corredera P, Hernanz ML, Hernanz J. Development of fiber optic hydrogen sensors for testing nuclear waste repositories. Sensor Actuator B Chem 2005;107:113–20.
[27] Lo C, Tan S-W, Wei C-Y, Tsai J-H, Lour W-S. "Sensing properties of resistive-type hydrogen sensors with a Pd–SiO2 thin-film mixture. Int J Hydrogen Energy 2013;38(1):313–8. https://doi.org/10.1016/j.ijhydene.2012.10.051.
[28] Hayashi Y, Yamazaki H, Ono D, Masunishi K, Ikehashi T. Investigation of PdCuSi metallic glass film for hysteresis-free and fast response capacitive MEMS hydrogen sensors. Int J Hydrogen Energy 2018;43(19):9438–45. https://doi.org/10.1016/j.ijhydene.2018.03.149.
[29] H El M, Domingue F, Palmisano V, Boon-Brett L, Post MB, Rivkin C, Burgess R, Buttner WJ. Assessment of commercial micro-machined hydrogen sensors performance metrics for safety sensing applications. Int J Hydrogen Energy 2014;39(9):4664–73. https://doi.org/10.1016/j.ijhydene.2014.01.037.
[30] Chou P-C, Chen H-I, Liu I-P, Chen C-C, Liou J-K, Lai C-J, Liu W-C. Hydrogen sensing characteristics of Pd/SiO2-nanoparticles (NPs)/AlGaN metal-oxide-semiconductor (MOS) diodes. Int J Hydrogen Energy 2014;39(35):20313–8. https://doi.org/10.1016/j.ijhydene.2014.10.022.
[31] Hecht ES, Panda PP. Mixing and warming of cryogenic hydrogen releases. Int J Hydrogen Energy 2018. https://doi.org/10.1016/j.ijhydene.2018.07.058.
[32] Settles GS, Hargather MJ. A review of recent developments in schlieren and shadowgraph techniques. Meas Sci Technol 2017;26.
[33] Buttner, W. and Ciotti, M., "Empirical profiling of cold hydrogen plumes formed from venting of LH2 storage vessels.
[34] Fuel Cell and hydrogen Joint undertaking, project PRESLHY (Pre-Normative research for safe use of liquid hydrogen). 2018.
[35] Hecht E, Panda P. Mixing and warming of cryogenic hydrogen releases. Int J Hydrogen Energy 2018. https://doi.org/10.1016/j.ijhydene.2018.07.058.
[36] Hydrogen. Fuel cells & infrastructure Technologies program multi-year research, development and demonstration plan, planned program activities for 2005–2015. U.S. DOE Office of Renewable Energy and Efficiency (EERE; 2005.
[37] IEC 60079-10-1 Explosive atmospheres – Part 10: classification of hazardous areas – explosive gas atmospheres. Edition vol. 2.0, 2015-09.
[38] LaChance JL, Brown J, Middleton B, Robinson D. Data for the use in quantitative risk analysis of hydrogen refueling stations. In: National hydrogen association meeting, Sacramento, CA, March 30 - April 3; 2008.
[39] HyApproval WP4 Safety. "Agreement on required modelling tools & techniques for risk assessments and simulations, accident scenarios, credible leak rates", V1.2 Final. 15 May 2007.
[40] Canadian hydrogen airport project, risk assessment and FMECA methodology. 2009-2011.
[41] HyQRA benchmark hydrogen fueling station: scenario definition. Workshop; 28 November 2008.
[42] Howard GW, Tchouvelev AV, Cheng Z, Agranat VM. Defining hazardous zones – electrical classification distances. ICHS2005; September 2005.
[43] Kikukawa S. Consequence analysis and safety verification of hydrogen fueling stations using CFD simulation. IJHE 2008;33:1425–34.
[44] Michael R. Swain, Eric S. Grilliot and Matthew N. Swain: Risks incurred by hydrogen escaping from containers and conduits. NREL/CP-570-25315. Proceedings of the 1998 U.S. DOE Hydrogen Program Review.
[45] Global technical regulation No. 13–Global technical regulation on hydrogen and fuel cell vehicles United Nations. 2013. p. 115. ECE/TRANS/180/Add.13.
[46] Buttner W, Rivkin C, Burgess R, Hartmann K, Bloomfield I, Bubar M, Post M, Boon-Brett L, Weidner E, Moretto P. Hydrogen monitoring requirements in the global technical regulation on hydrogen and fuel cell vehicles. Int J Hydrogen Energy 2017;42(11):7664–71. https://doi.org/10.1016/j.ijhydene.2016.06.053.
[47] Post Mathew, Burgess Robert, Rivkin Carl, William J, Kathlen O'Malley Buttner, Ruiz Antonio. Onboard hydrogen/Helium sensors in support of the global technical regulation: an assessment of performance in fuel Cell electric vehicle crash tests. 2012. NREL/TP-5600-56177.
[48] Buttner William, Weidner Eveline, Burgess Robert, Schmidt Kara, Wright Hanna, Rivkin Carl, Ortiz Cebolla Rafeal, Bonato C, Moretto Pietro, Hill Laura, Will James C. Hydrogen safety sensor performance and use gap analysis. In: Proceedings of the 7th international conferenceon hydrogen safety, The 7th international conference on hydrogen safety. Hamburg, Germany: ICHS); 2017.
[49] Buttner W, Ciotti M, Hartmann K, Schmidt K, Wright H, Schmidt K. Empirical profiling of cold hydrogen plumes formed from venting of LH2 storage vessels. Adelaide, Australia, ICHS2019. 2019.

Please cite this article as: Tchouvelev AV et al., Development of risk mitigation guidance for sensor placement inside mechanically ventilated enclosures – Phase 1, International Journal of Hydrogen Energy, https://doi.org/10.1016/j.ijhydene.2020.09.108

[50] Agranat V, Cheng Z, Tchouvelev A. CFD modeling of hydrogen releases and dispersion in hydrogen energy station. Proceedings of the 15th world hydrogen energy conference 2004.
[51] NREL National Wind Technology Center (NWTC), (see https://www.nrel.gov/about/nwtc.html).
[52] Birch AD, Brown DR, Dodson MG, Swaffield F. The structure and concentration decay of high pressure jets of natural gas. Combust Sci Technol 1984;36:249–61.
[53] Menter F. Two-equation eddy-viscosity turbulence models for engineering applications. AIAA J 1994;32:1598–605.
[54] Langtry R, Menter F. Correlation-based transition modeling for unstructured parallelized computational fluid dynamics codes. AIAA J 2009;47:2894–906.

Please cite this article as: Tchouvelev AV et al., Development of risk mitigation guidance for sensor placement inside mechanically ventilated enclosures – Phase 1, International Journal of Hydrogen Energy, https://doi.org/10.1016/j.ijhydene.2020.09.108